

# MISA Lab 3 Report

## Atlas based segmentation

Colin Tenorio C.G., Ulin Briseño E.Y.

<sup>1</sup> EPS, University of Girona, Spain.

*carmencolinten@gmail.com, eulinbriseno@gmail.com*

**Key words:** Atlas, Segmentation, Registration, Brain, EM

### Introduction

Atlas-based segmentation is a powerful generic technique for the automatic delineation of objects in volumetric images, taking into account neighborhood relationships between several different structures. Normal and abnormal brains can be segmented by registering the target image with an atlas. Here, an atlas is defined as the combination of an intensity image (template) and its segmented image (the atlas labels). After registering the atlas template and the target image, the atlas labels are propagated to the target image. We define this process as atlas-based segmentation. With this strategy, the segmentation process relies on a registration process that aims to estimate the anatomical differences between the atlas and the input image volumes.

### Objectives

This is the second part of Atlas-based segmentation. In this lab, we will perform segmentation using the atlas from the first part. We will also use the EM algorithm from the previous lab. The objective of this lab is to use our Atlas to segment the different brain tissues: CSF, WM, and GM. The main goals are:

1. To understand the segmentation algorithm when integrating atlas information, to design, analyze, and implement the algorithm.
2. To test the algorithm with the provided images, study the problems, explore possible improvements, and evaluate the results using the provided ground truth and the Dice Similarity Coefficient (DSC).

### Methodology

#### Data

The training dataset used to construct the atlas comprises 15 MRI volumes obtained from clinical data provided by the professors. The testing dataset consisted of 20 volumes. As complementary, a standar Atlas was provided: the standard Montreal Neurological Institute (MNI) Atlas, including the Atlas and the template image.

## Registration

For the registration process, our target images are the testing volumes. We need to register both atlases to the space of the target image. In this project, we found that Parameter10 (affine) and Parameter25 (rigid) produced the most effective registrations when used in combination. These parameters are available for reference on the following GitHub repository: <https://github.com/SuperElastix/ElastixModelZoo/tree/master/models>. For most of the parameters, it was essential to include the following lines to ensure proper configuration:

```
(ResultImagePixelType "float")
(ResultImageFormat "nii")
```

For this project, we used the Elastix software to perform the registration. To run the software, we need to define the arguments as input:

1. **Moving Image Path:** This argument represents the path to the image that requires registration. The moving image serves as the subject of the alignment.
2. **Fixed Image Path:** The path to the fixed image, on the other hand, serves as the reference or target image for registration.
3. **Transformation Parameters:** These parameters act as the set of instructions that dictate how the moving image should be transformed to optimally align with the fixed image.
4. **Result Path:** The path to save the final result.

### Label Propagation

To propagate labels into a common space, we employ the Transformix tool integrated into the Elastix software. This process involves three essential parameters:

1. **Input Image Path:** This parameter designates the file path to the image requiring registration, which serves as the subject of alignment.
2. **Transformation Parameters:** These are the transformation parameters acquired in the previous registration step, defining the transformation model that guides the alignment of labels to the common space.
3. **Result Path:** This specifies the directory where the final transformed labels will be stored.

## Atlas Segmentation:

### Segmentation without EM

The atlas is employed within a Bayesian framework to segment the different brain tissues. In this case, the true label (the segmentation or set of labels) is denoted by  $X$ , and the target image (a dataset of intensity values) is denoted by  $Y$ . The problem consists of estimating the label  $X$  that best explains the given observation  $Y$ .

The segmentation  $X$  is estimated by maximizing the global a posteriori probability  $P(X|Y)$ , searching for the most probable labeling given the image  $Y$  and some prior model. Using Bayes' theorem, the posterior probability to be maximized can be written as  $P(Y|X)P(X)$ .

For each structure, a histogram of intensity values is built by considering the voxels of the MRI volumes that belong to it, using the manual segmentations. On the other hand, the probability distribution  $P(X)$  is given by the probabilistic atlas once it has been mapped onto the target space using the same registration procedure used in its construction.

### Tissue Models:

Segmentation can be achieved using intensity information alone. In this case, we constructed tissue models where each intensity is assigned a probability for each of the tissue classes. The segmentation is obtained by maximizing the likelihood:

$$P(X|Y) = \text{argmax}P(Y|X) \quad (1)$$

representing the probability of belonging to each of the classes (CSF, WM, GM) based on the intensity value.

### Label Propagation:

Segmentation can be performed using only position information, utilizing the probability distribution  $P(X)$ . In this case:

$$P(X|Y) = \text{argmax}P(X) \quad (2)$$

representing the probability of belonging to each of the classes (CSF, WM, GM) based on its position.

### Tissue Models and Label Propagation:

Segmentation can be accomplished using both position and intensity information. In this case:

$$P(X|Y) = \text{argmax}P(X)P(Y|X) \quad (3)$$

indicating the probability of belonging to each of the classes based on position and intensity information.

### Segmentation with EM: Atlas Information as Initialization

In this section, we utilized the EM algorithm for segmentation with various initializations. The EM algorithm can be initialized in different ways for segmentation, incorporating both intensity and position information. The following initializations were employed:

- Using intensity information.
- Using k-Means as initialization.
- Using tissue models as initialization.
- Using label propagation initialization from atlas probabilistic maps.

In these cases, the probability maps act as weights, assisting in estimating the initial parameters (mean, covariance, and priors) for each cluster in the Gaussian Mixture.

In this part we took the previous code for our EM, some necessary alterations are needed. Because our other implementation calculated the values from the given data; however in the implementation of the Atlas segmentation the posteriors data is given by the probabilities of our own atlas. The implementation used the previous core of the project to build this integration. So, for the new integration of

the data is pass as the posteriors of the calculations, the tissue model is used for calculating a probability map for the posteriors, and we used some control flags to used the multiplication of the into and after. The result of this part of the code is discussed in the next parts.

### Segmentation with EM: Atlas in the Algorithm

The atlas information can be included in the EM algorithm in two ways:

**Into EM:** Utilizing the membership weight of data point  $x_i$  in cluster  $k$  given parameters  $\Theta$ , defined as:

$$w_{ik} = p(z_{ik} = 1 | x_i, \Theta) = \frac{p_k(x_i | z_k, \theta_k) \cdot \alpha_k}{\sum_{m=1}^K p_m(x_i | z_m, \theta_m) \cdot \alpha_m} \quad (4)$$

This equation is modified by multiplying it by the probability from the atlas for each class.

**After EM:** After obtaining the final probability maps (posteriors) from the EM algorithm, these maps are multiplied by the probability maps of the atlas.

## Implementation

### Registration

For the registration part, we utilized the same parameters as in the previous lab, as they provided excellent results. In this case, each test image served as a fixed image, as both atlases (MNI and Our Atlas) needed to be moved. The atlas templates were the moving images. Subsequently, the same process was applied to the atlas probability maps using the parameter maps. Label propagation was then performed for each tissue.

### Segmentation Without EM

For this part, three different segmentation approaches were employed:

**Tissue Models:** Segmentation using only intensity information. The highest probability from the tissue models for each pixel intensity value was used to assign the corresponding class.

**Label Propagation:** Segmentation using only position information. The maximum probability for each pixel position was assigned as the class for that pixel.

**Tissue Models and Label Propagation:** Segmentation using both intensity and position information. Both probabilities were multiplied, creating a matrix of probabilities for each pixel, and the maximum probability after multiplication was obtained. In all cases, the brain mask was used to segment only the regions with tissues.

### Segmentation with EM

The modifications to the EM algorithm can be categorized into two major components: the initialization of the data and the optimization of weights, incorporating the "Into" and "After" atlas strategies. The first significant alteration involves discontinuing the calculation of initial values from the data distribution. Instead, we utilize the posteriors derived from the probabilities of the atlas. The information from the probabilistic atlas is passed directly as posteriors, maintaining compatibility with the data structure within the EM algorithm. For the tissue model, it was necessary to create a probabilistic matrix from the intensities within the original data.

The subsequent integration of the atlas is in the "Into" phase, where a multiplication occurs within every expectation phase. This integration provides spatially informed priors, guiding the probability estimates based on known anatomical structures and locations. The final integration is the "After" phase, involving a multiplication of the last probabilities. This step refines the segmentation results by aligning them more closely with expected anatomical structures.

## Results

### Registration

For the registration process, examples of the results are shown in Fig. 1 and 2, using a testing volume as a fixed image. The figures display the original atlases, the target testing image, and the output of the registration. Subsequently, the label propagation is applied to each map of the original atlas, transforming them to the new space of the target image. This incorporation of spatial information from the original atlases into a new, unknown volume enhances our ability to segment tissues effectively.

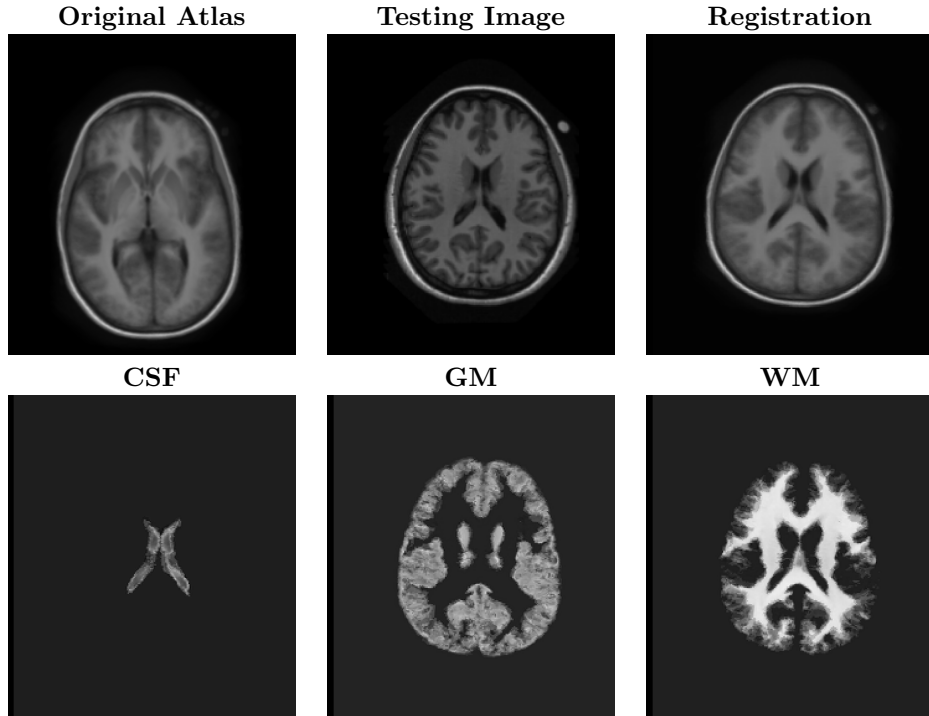


Figure 1: Example of Registration using Our Atlas as moving Image and a testing volume as Fixed image

### Segmentation without EM Algorithm

For each testing volume in the dataset, we conducted the segmentation of various brain tissues. Specifically, we obtained 20 segmentations for each method: Tissue Models, using Our Atlas, using Atlas

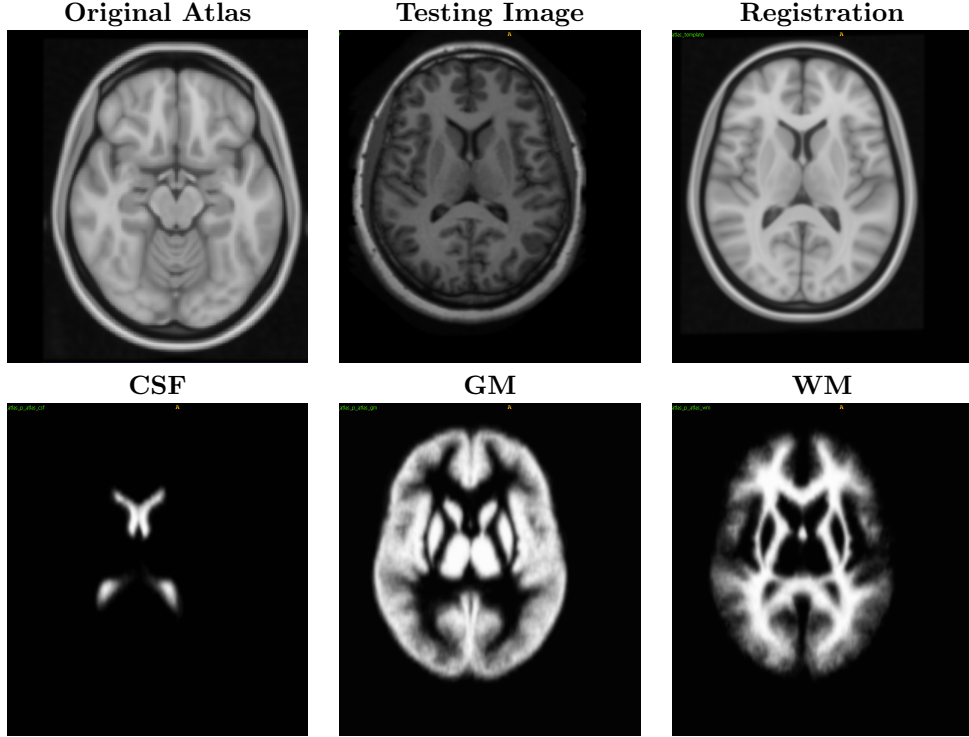


Figure 2: Example of Registration using the MNI Atlas as moving Image and a testing volume as Fixed image

MNI, Using Tissue Models and MNI Atlas, and finally, Tissue Models and Our Atlas.

The quantitative results are presented in Table 1. Overall, the results indicate that the utilization of Tissue Models improves segmentation performance. Since the tissue models were obtained from the same set of volumes used for training and testing, they exhibit significant similarities, contributing to enhanced performance for this dataset. Additionally, Our Atlas demonstrated the least favorable results, with a maximum DICE mean score of 0.606 for GM. This could be attributed to challenging testing cases as target images or factors in the atlas-building process, such as parameter selection. It is noteworthy that CSF consistently displayed the lowest DICE mean score across all segmentation methods. Combining tissue models and Our Atlas yielded the highest scores among the various methods, with DICE mean scores above 0.65 for all three classes.

The qualitative results for this approach are depicted in Fig. 3. From top to bottom, the images show the Original Image T1, Ground Truth Label, and the segmentation results using Tissue Models, Our Atlas, MNI Atlas, Tissue Models and MNI ATLAS, and Tissue Models and Our Atlas for four different volumes. In the quantitative analysis, it is evident that segmenting the CSF poses a greater challenge compared to other brain tissues. Notably, the combination of tissue models and Our Atlas demonstrates superior results when compared to the ground truth images. Conversely, the standalone use of Our Atlas yields less favorable outcomes, particularly in the segmentation of white and gray matter. This discrepancy suggests that the integration of tissue models enhances the segmentation accuracy of Our Atlas, highlighting the complementary nature of intensity-based information and atlas-

guided spatial knowledge.

Table 1: Mean DICE scores of the volumes with different segmentation methods

Segmentation Method	CSF	GM	WM
Tissue Models	0.310	0.876	0.838
Our Atlas	0.451	0.606	0.479
Atlas MNI	0.498	0.652	0.721
Tissue Models + Atlas MNI	0.419	0.845	0.893
Tissue Models + Our Atlas	0.657	0.855	0.898

## Segmentation EM algorithm

For quantitative results, the table 2 displays the mean DICE scores for the three brain tissues (CSF, GM, WM) obtained through different initializations in the EM algorithm. The results indicate that Our Atlas exhibits the lowest mean DICE score for CSF, while achieving higher scores for GM and WM. K-Means and MNI Atlas initializations show improved performance for CSF compared to Our Atlas, but still lag behind in overall accuracy. Tissue Models and MNI Atlas demonstrate comparable mean DICE scores, with Tissue Models yielding slightly better results for CSF. These findings emphasize the importance of the chosen initialization method in influencing the segmentation outcomes.

The table 3 presents DICE scores for CSF, GM, and WM after and into the EM algorithm using Our Atlas. The results reveal that the segmentation performance improves for CSF, GM, and WM in the "After" stage compared to the "Into" stage. The DICE scores indicate very low accuracy for CSF in both methods after and Into, while GM and WM show improved performance in the Into.

In the case of qualitative results, the figures (Fig. 4, 5, 6, and 7) illustrate examples of testing volumes using the EM algorithm with different initializations: K-Means, Our Atlas, MNI Atlas, and Tissue Models. The figures present segmentation results into and after the EM algorithm.

CSF appears to be the most challenging class to segment consistently across all cases. Comparing the results with K-Means initialization to those with atlas information, there is an observable improvement in segmentation when incorporating atlas information. The addition of tissue models further enhances segmentation results.

Interestingly, when using only Our Atlas, the segmentation results are challenging, especially in distinguishing between GM and WM. This suggests that the integration of spatially informed priors and the combination of intensity and position information contribute to improved segmentation outcomes.

For the qualitative results involving atlas information in both intro and after steps, refer to Fig. 8. The figures provide examples of segmentation results for various testing volumes when incorporating atlas information into and after the EM algorithm.

While it may be challenging to thoroughly appreciate improvements or differences, it is noticeable that the labels change with each method, and the final segmentation differs from the ground truth. In these cases, the Into method appears to make an effort to better distinguish between WM and GM.

Table 2: Mean DICE scores of all the volumes using different initialization in the EM algorithm

Initialization	CSF	GM	WM
Our Atlas	0.106857	0.851527	0.830164
K-Means	0.212289	0.822132	0.809018
MNI_Atlas	0.252410	0.834133	0.779591
Tissue Models	0.252410	0.834133	0.779591

Table 3: Intro and After for the brains 1116 - 1128

Atlas_use	CSF	GM	WM
After	0.121238	0.673310	0.636561
Into	0.098685	0.659315	0.698520

## Time Tracking and Task

The project management is outlined in Fig. 9. The planned total time for the entire project was 12 hours, distributed across tasks such as initial atlas registration, data preparation for both EM and non-EM segmentation, and joint reporting. Initial atlas registration was assigned to Carmen, while Edwing handled the EM-related tasks. Report writing was a collaborative effort.

In reality, the EM task proved more time-consuming than anticipated. Challenges, such as code debugging, data ingestion errors, and unexpected issues, led to an extension of the initially allocated time for this task. Consequently, this had an impact on the overall project timeline and delivery.

The time tracking and task allocation, as illustrated in the project timeline, underscore the importance of contingency planning and flexibility in adapting to unforeseen challenges during the project's execution.

## Discussion

The segmentation results obtained without using the Expectation-Maximization (EM) algorithm offer valuable insights into the effectiveness of different methods. Tissue Models, relying on intensity information alone, demonstrated significant contributions to segmentation accuracy. The shared characteristics between the training and testing datasets played a pivotal role, making Tissue Models a robust approach for this specific dataset.

Surprisingly, Our Atlas exhibited suboptimal performance, with DICE mean scores trailing behind other methods. Possible factors contributing to this outcome include challenging testing cases, intricacies in the atlas-building process, or suboptimal parameter choices. Notably, consistently lower DICE scores for CSF across all methods may indicate inherent challenges in accurately segmenting this tissue

type.

The combination of Tissue Models with Our Atlas yielded the most favorable outcomes, suggesting a synergistic effect. This underscores the importance of integrating both intensity-based information and atlas-guided segmentation for improved accuracy. However, further investigation and optimization of the atlas-building process may be needed to enhance the performance of Our Atlas.

The segmentation results incorporating the Atlas information via the Expectation-Maximization (EM) algorithm reveal a nuanced interplay of factors influencing accuracy. The effectiveness of this approach heavily relies on the quality of the atlas, the chosen parameters, and the number of iterations. One notable challenge observed in our implementation is the substantial overlap in the White Matter (WM) and Cerebrospinal Fluid (CSF) regions, contributing to confusion in the segmentation.

To address this issue, implementing a mask to filter out irrelevant information during EM iterations could prove beneficial. By selectively focusing on regions of interest, the segmentation process may yield more accurate and meaningful results, particularly in areas with considerable tissue overlap.

Additionally, investigating the impact of varying the number of iterations in the EM algorithm is crucial. Finding the optimal balance between computational efficiency and segmentation accuracy is essential. Too few iterations may lead to premature convergence and suboptimal results, while too many may introduce unnecessary computational burden without significant improvement.

While the project exhibits consistency across different domains, such as intensity-based tissue models and spatially informed atlas-guided segmentation, there remains substantial room for improvement. Future work could explore parameter tuning, refinement of atlas-building processes, and more sophisticated methods to address the WM and CSF overlap. These endeavors aim to elevate the segmentation accuracy and robustness of the overall pipeline.

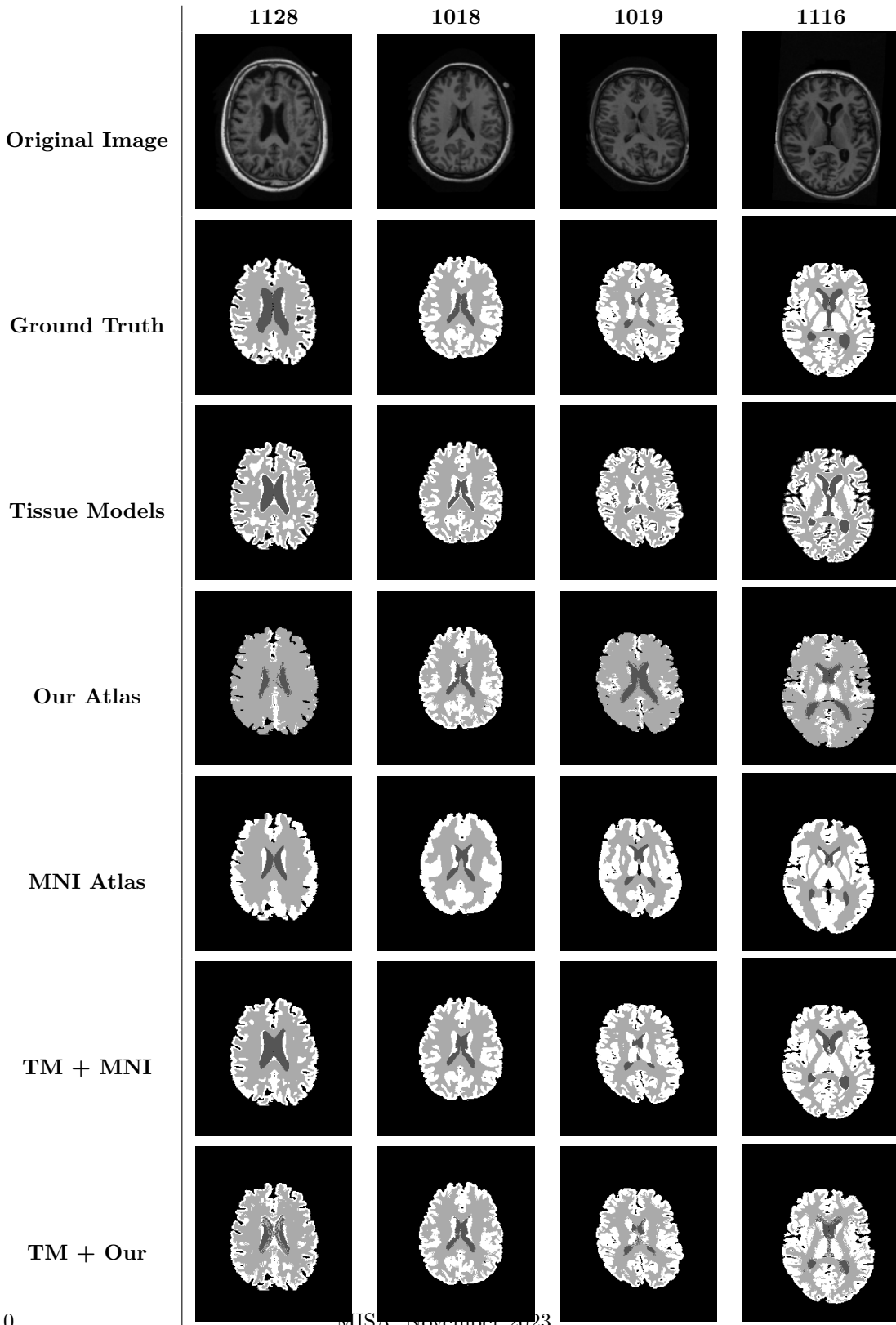


Figure 3: Example of Brain tissue segmentations using Position and Intensity information. From both Atlases: Our Atlas and MNI Atlas.

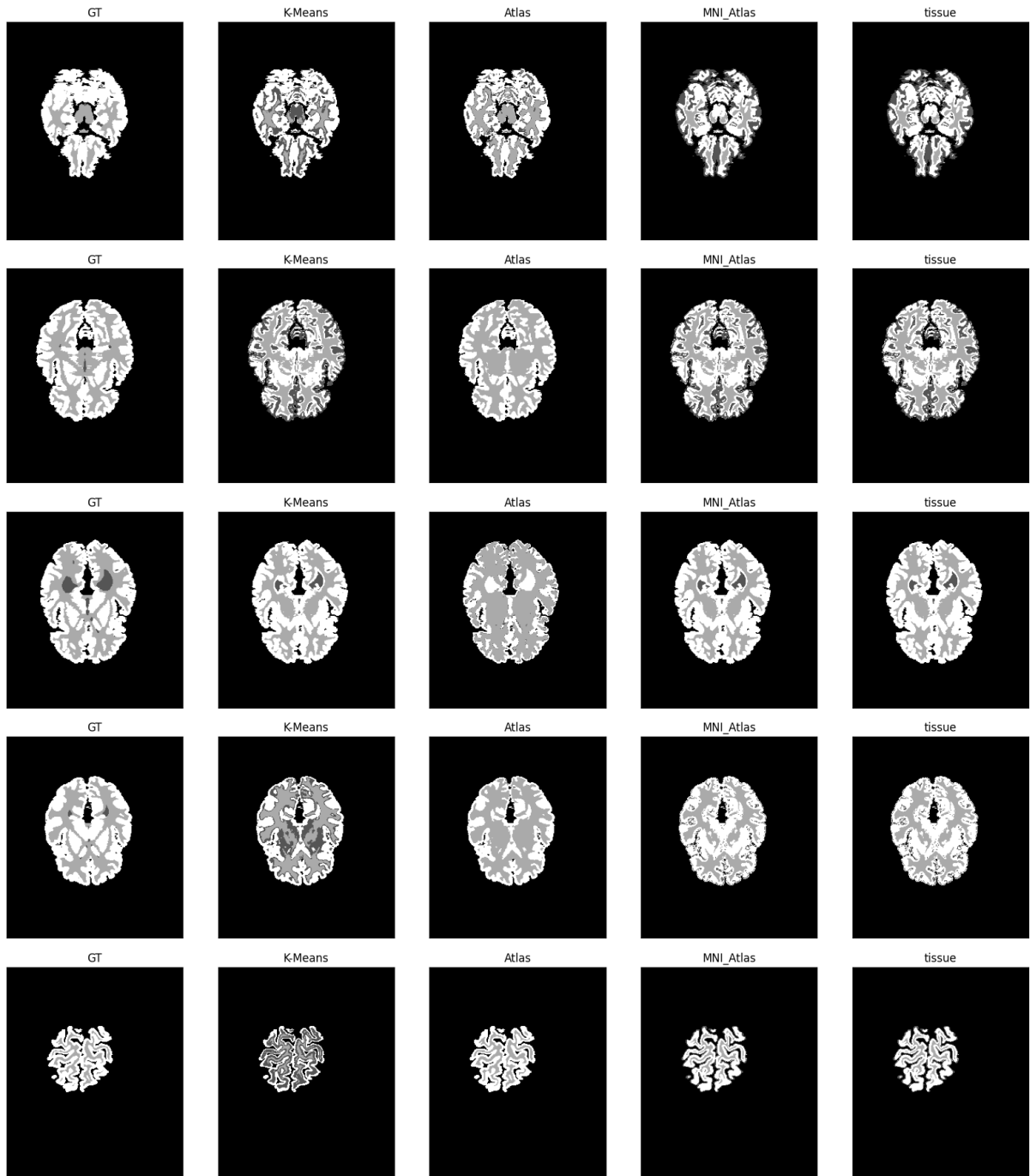


Figure 4: Example of segmentation results of EM 1004 - 1019. When changing the initialization method in the EM algorithm: K-means, Our Atlas, MNI Atlas and Tissue Models.

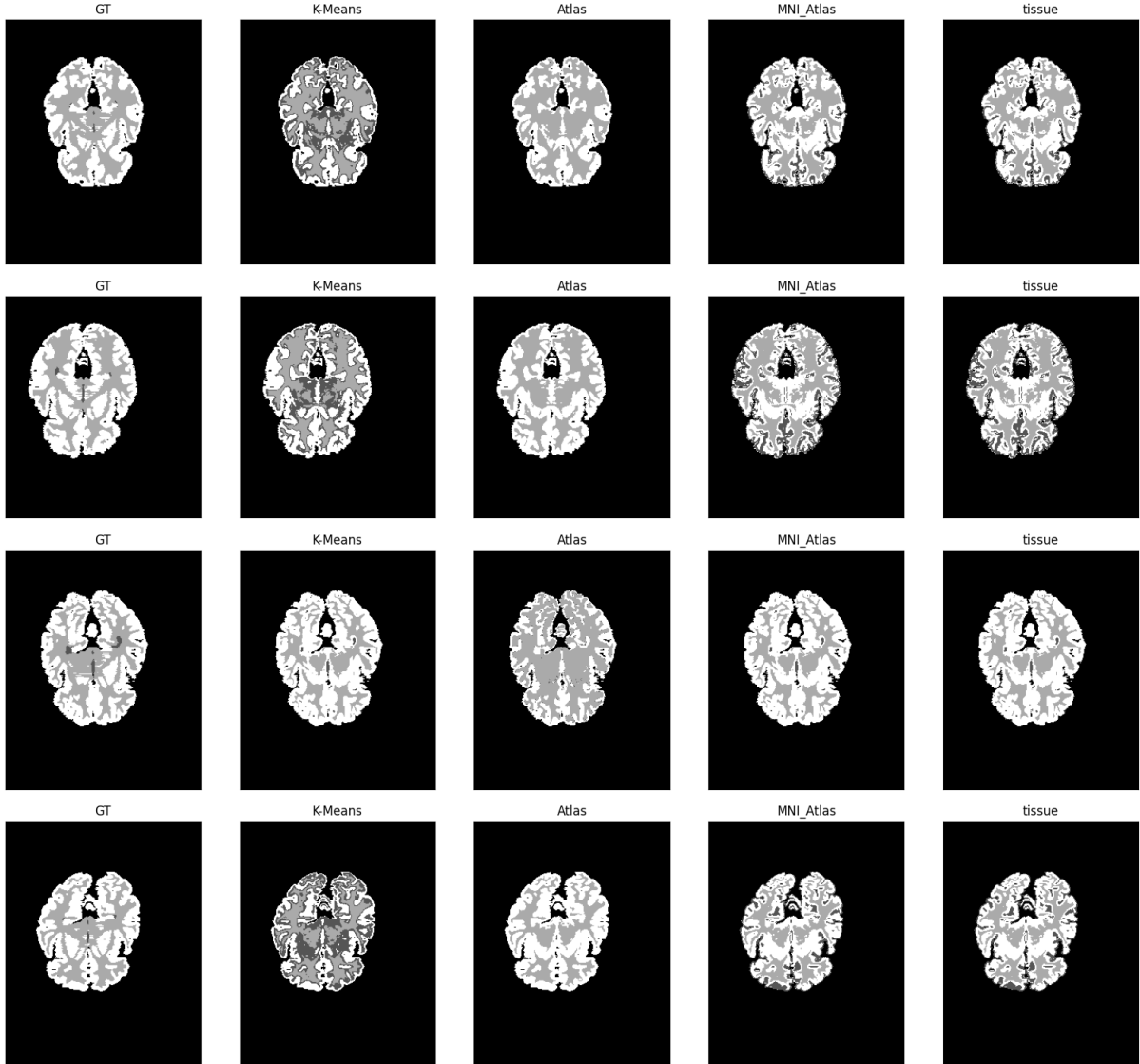


Figure 5: Example of segmentation results of EM 1023 - 1039. When changing the initialization method in the EM algorithm: K-means, Our Atlas, MNI Atlas and Tissue Models.

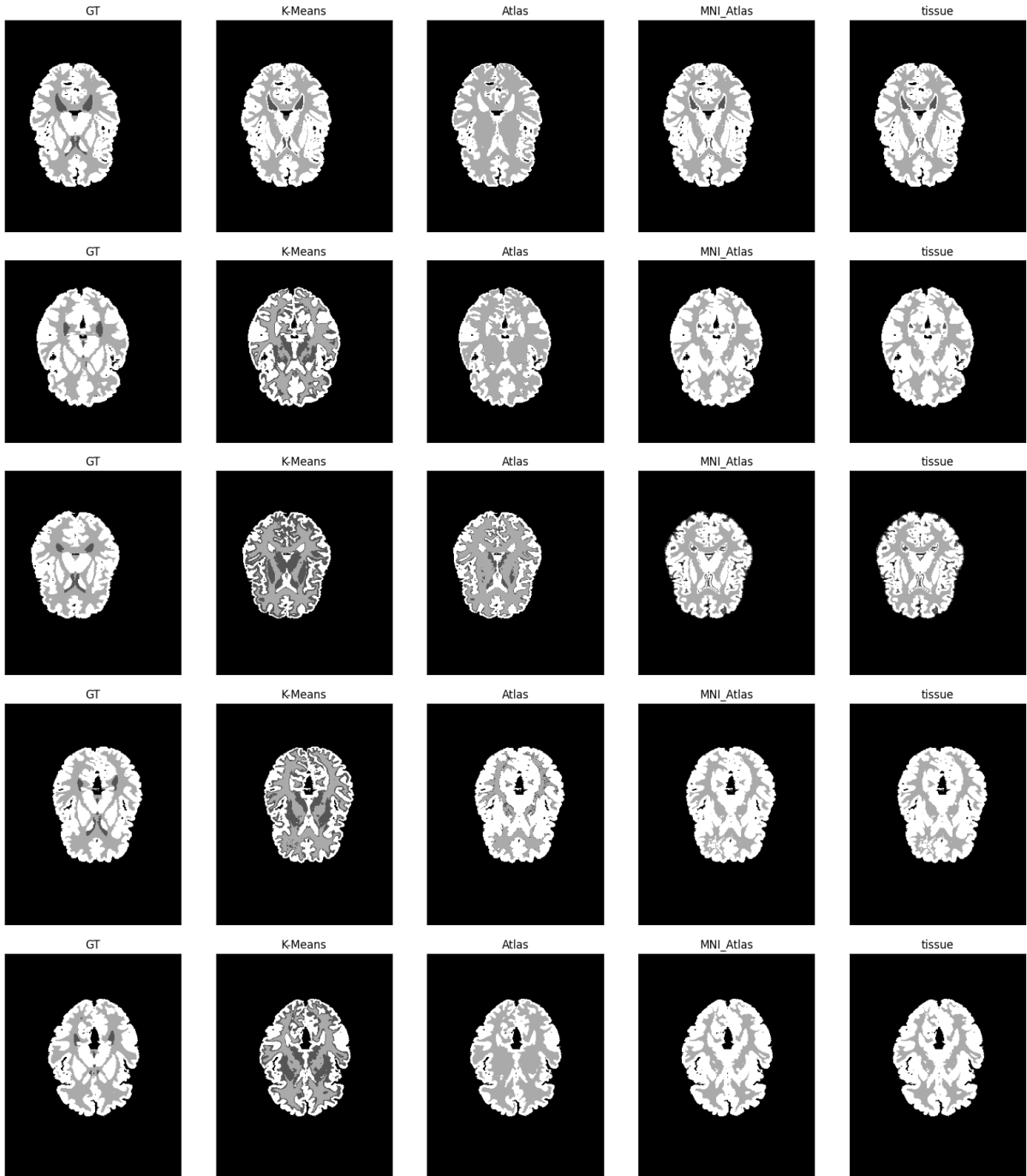


Figure 6: Example of segmentation results of EM 1101 - 1113. When changing the initialization method in the EM algorithm: K-means, Our Atlas, MNI Atlas and Tissue Models.

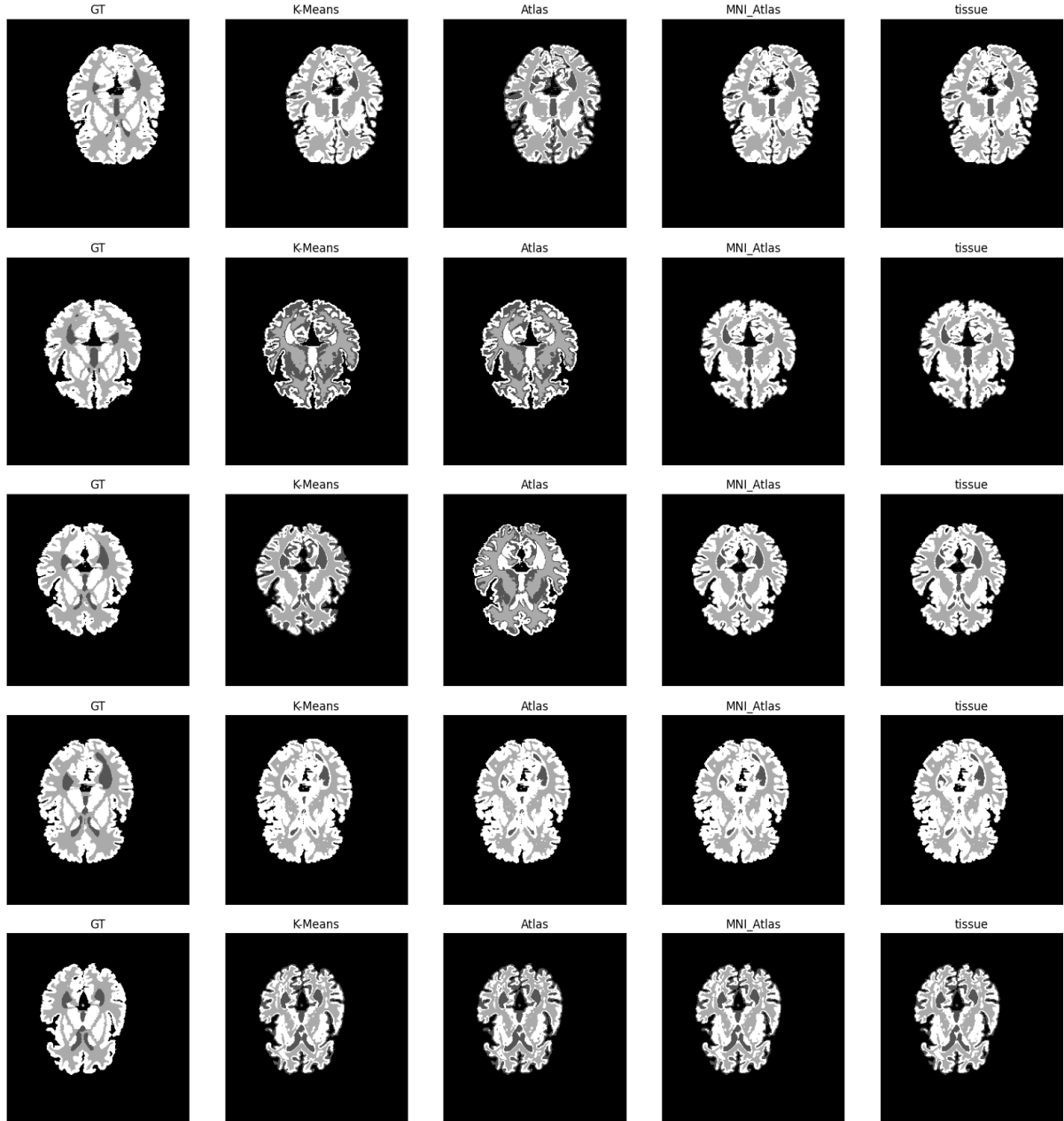


Figure 7: Example of segmentation results of EM 1116 - 1128. When changing the initialization method in the EM algorithm: K-means, Our Atlas, MNI Atlas and Tissue Models.

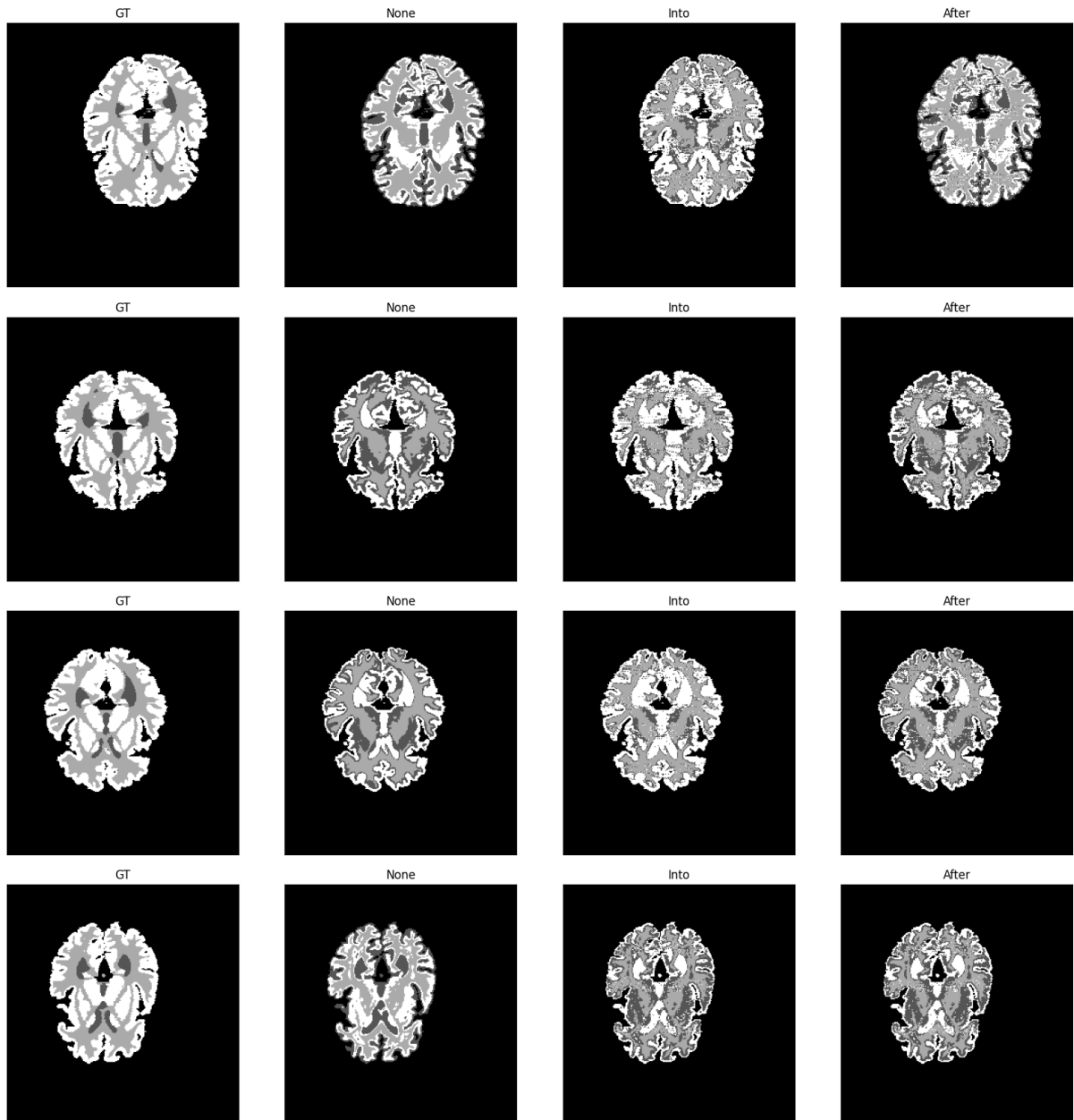


Figure 8: Example of segmentation results of EM and atlas information Intro and After

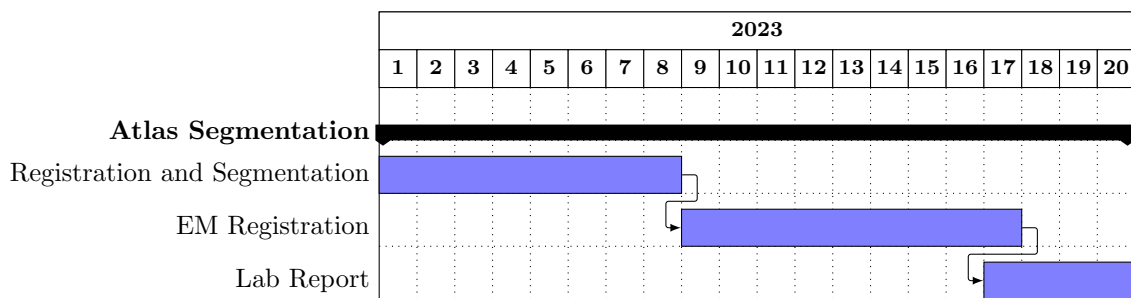


Figure 9: Gantt Chart for Project Atlas